FULL PAPER

PPS
www.rsc.org/pps

Autofluorescence properties of isolated rat hepatocytes under different metabolic conditions

Anna Cleta Croce,[a] Andrea Ferrigno,[b] Mariapia Vairetti,[b] Roberta Bertone,[a] Isabel Freitas[a] and Giovanni Bottiroli[a]

[a] *Histochemistry and Cytometry Section, IGM-CNR, Department of Animal Biology, Piazza Botta, 10, 27100 Pavia. E-mail: leta@igm.cnr.it; Fax: +39 0382 506430; Tel: +39 0382 506428*

[b] *Department of Internal Medicine and Therapy, University of Pavia, Piazza Botta, 10, I-27100 Pavia, Italy*

Received 14th May 2004, Accepted 28th July 2004
First published as an Advance Article on the web 31st August 2004

The contribution of endogenous fluorophores – such as proteins, bound and free NAD(P)H, flavins, vitamin A, arachidonic acid – to the liver autofluorescence was studied on tissue homogenate extracts and on isolated hepatocytes by means of spectrofluorometric analysis. Autofluorescence spectral analysis was then applied to investigate the response of single living hepatocytes to experimental conditions resembling the various phases of the organ transplantation. The following conditions were considered: 1 h after cells isolation (reference condition); cold hypoxia; rewarming–reoxygenation after cold preservation. The main alterations occurred for NAD(P)H and flavins, the coenzymes strictly involved in energetic metabolism. During cold hypoxia NAD(P)H, mainly the bound form, showed an increase followed by a slow decrease, in agreement with the inability of the respiratory chain to reoxidize the coenzyme, and a subsequent NADH reoxidation through alternative anaerobic metabolic pathways. Both bound/free NAD(P)H and total NAD(P)H/flavin ratio values were altered during cold hypoxia, but approached the reference condition values after rewarming–reoxygenation, indicating the cells capability to restore the basal redox equilibrium. A decrease of arachidonic acid and vitamin A contributions occurred after cold hypoxia: in the former case it may depend on the balance between deacylation and reacylation of fatty acids, in the latter it might be related to the vitamin A antioxidant role. An influence of physico-chemical status and microenvironment on the fluorescence efficiency of these fluorophores cannot be excluded. In general, all the changes observed for cell autofluorescence properties were consistent with the complex metabolic pathways providing for energy supply.

Introduction

Biological substrates submitted to excitation in the UV-Visible range give rise to an autofluorescence emission. This phenomenon is due to the presence of biomolecules acting as endogenous fluorophores, which can be involved either in the histological organization of the tissues, such as constitutive proteins, or in metabolic processes, such as nicotinic coenzymes, flavins, lipopigments and porphyrins.[1–3]

The features of autofluorescence emission, in terms of amplitude and spectral shape, depend on nature, amount, physico-chemical state, intratissue distribution of endogenous fluorophores, and on the properties of the microenvironment, in close relationship with the morphological and metabolic conditions of cells and tissues. Autofluorescence can thus be considered as an intrinsic parameter of biological substrates that can be exploited for a real time investigation of tissue and cell morpho-functional state. The earliest application of autofluorescence analysis concerned the study of the dynamic evaluation of metabolism directly in single living cells. The reduced pyridine nucleotide NAD(P)H was localized and quantitatively evaluated in intact cells through its autofluorescence emission, which showed changes, for example, in dependence on the aerobic or anaerobic conditions, or on glucose supply.[4,5]

At present, autofluorescence-based techniques are widely investigated for the direct, *in situ* diagnosis of tissue diseases, in particular neoplasias and differentiated condition.[6–13] Interest is rising also on the study of the relationship between the metabolic engagement and tissue autofluorescence properties, in view of developing a method to monitor organ functional conditions during the different phases of transplantation. The clinical transplantation procedure consists in: withdrawal from the donor, preservation, grafting in the recipient. In the case of liver, the preservation phase, based on cold hypoxia and nutrient depletion, and the reperfusion following grafting in the recipient can induce major liver injuries, which are possible causes of transplant dysfunction.[14–16]

The alterations occurring in the liver functional conditions modify the content and physico-chemical state of the endogenous fluorophores engaged in the metabolic processes, thus affecting tissue autofluorescence properties. Therefore, autofluorescence spectroscopic analysis is expected to provide a valid tool for a real time monitoring of liver functional condition. Studies are reported in the literature on the relationship between the autofluorescence properties of hepatocytes – attributable to the coenzymes linked to the energetic metabolism, such as NAD(P)H and flavins – and the redox state of the cells.[17] A relationship was also evidenced between the hypoxic conditions and tissue autofluorescence properties, both *in vivo* and *ex vivo* in the explanted intact liver.[18–19]

Actually, the multiple and diversified functions exerted by the organ – biosynthesis, catabolism and detoxification – imply complex interactions between various metabolic paths which involve the contribution of endogenous fluorophores other than NAD(P)H and flavin coenzymes, and namely fatty acids, lipopigments, vitamins, biliary salt derivatives. In this work a spectrofluorometric study on liver extracts and on isolated hepatocytes was performed with the aim to characterize the nature of the fluorophores and the dependence of their contributions on the experimental conditions mimicking those of the various phase of the organ transplantation.

DOI: 10.1039/b407358d

Materials and methods

Chemicals

Vitamin A (All-*trans*-retinoic acid) and arachidonic acid, as pure compounds, were dissolved directly in chloroform (0.5 mg ml^{-1}) and diluted to 0.025 mg ml^{-1} for spectrofluorometric analysis. NADH and Flavin adenine dinucleotide (FAD) solutions were prepared as already described.[1] Briefly, NADH was dissolved at the concentration of 10 mg ml^{-1} in tris(hydroxymethyl)aminomethane (TRIS) buffer (0.1 M, pH 8), because NADH is stable under basic conditions. This solution was diluted 1 : 1 with the same buffer or with an alcohol dehydrogenase solution (E.C. 1.1.1.1, 10 mg ml^{-1} in the same buffer), for the free and bound conditions, respectively. FAD was dissolved in phosphate buffer (0.05 M, pH 7.4) at the concentration of 5 mg ml^{-1}. Collagenase (Type I; E.C. 3. 4. 24. 3), and all the chemicals were purchased from Sigma Chem. Co., MO, USA.

Liver tissue homogenates

The tissue samples were collected from livers of male Wistar rats (250–300g; Harlan-Nossan, Correzzana, Italy). The animals had free access to water and food. The use and care of animals in this experimental study was approved by the Italian Ministry of Health and by the University Commission for Animal Care following the criteria of Italian National Research Council. Rats were anaesthetized with ip injection of penthobarbital (40 mg kg^{-1}). The liver samples (about 150 mg each) were quickly removed and frozen immediately in liquid nitrogen and stored at −80 °C, until they were processed for homogenisation. A moderate ionic strength homogenisation medium was used consisting in: an anti-oxidant (d*l*-dithiothreitol, 20 mM), a proteolytic inhibitor (phenylmethane sulfonyl fluoride, 1 mM), a chelating agent (EDTA, 5 mM) and a detergent for protein solubilization (Triton X-100, 0.01% w/v) dissolved in 0.005 M phosphate buffer (pH 7.4), according to a previously-described procedure.[8] Tissue samples, immersed in the medium (150 tissue mg : 1 medium ml), were homogenised using an Ultra Turrex T25 tissue homogeniser (Janke and Kunker, Stauffen, Germany). Homogenates were centrifuged at 5000 g for 15 min. The supernatant acqueous phase was collected and submitted to spectral analysis, after a 1 : 100 dilution in the same buffer in the absence of Triton, so that the interference of the buffer components with fluorescence measurements is negligible.[8]

For the extraction of the lypophilic components, the pellet was resuspended in 3 ml of a mixture of chloroform–water (2 : 1), shaken vigorously, and centrifuged. The organic solvent phase at the bottom of the tube and the unsoluble material were collected separately and submitted to spectral analysis.

Isolated hepatocytes

Hepatocytes were isolated by collagenase perfusion of rat livers as described by Moldeus *et al.*[20] The cell viability at the beginning of the experiments was 85–90%, as estimated by means of Trypan blue exclusion test. After isolation, cells were suspended in a Williams E medium supplemented with 0.1 mg ml^{-1} streptomycin, 100 U ml^{-1} penicillin and 5 mM *N*-(2-hydroxyethyl)-piperazine-*N*′-(2-ethanesulfonic acid) (HEPES), pH 7.4, and plated on Petri dishes (5×10^5 ml^{-1}), each one containing a polylysine-coated 30 mm ∅ glass coverslip. Cells were maintained in an incubator at 37 °C for 1 h to allow cell attachment and equilibration. Subsequently, part of these slides were directly submitted to measurements (reference samples), and part submitted to hypoxic treatment prior measurement. In the latter case, hepatocytes were rinsed twice in phosphate saline buffer (PBS) and incubated in conventional University of Wisconsin solution, UW (ViaSpan®; Pomona, NY, USA).[21] The slides were mounted up-down in the chamber described below for the measurements at short, prefixed times, or kept up to 20 h in an anoxia chamber under N_2 saturation at 4 °C. At the end of the cold hypoxic phase, cells were incubated at 37 °C in Krebs–Henseleit buffer, saturated with a 95% O_2 and 5% CO_2 gas mixture (rewarming–reoxygenation condition) and submitted to measurements. Cell viability was monitored by measuring the activity of LDH relesed into the medium as described by Bergmeyer.[22] Maximal LDH release was determined after exposing the cells to 10% of Triton X-100 (50 μL into 2 ml medium). Cell death was 15 ± 2.7% and 40 ± 7.3% at the end of cold hypoxia and after rewarming reoxygenation phases, respectively (values are means ±SE, $n = 4$).

Cell morphology and glycogen content

The cell morphology and glycogen content were investigated on hepatocyte reference samples, on hepatocytes at the end of cold hypoxia and after the rewarming–reoxygenation phase. Cells were fixed with 2% *p*-formaldehyde after the removal of the culture medium, and stained with conventional hematoxylin and eosin or periodic acid–Schiff (PAS) reactions.

Spectrofluorometric analysis

Excitation and emission spectra of aqueous and organic phases of liver homogenate were recorded by means of a SP-2 spectrofluorometer (Applied Photophysics, London, UK), equipped with a single-photon counting system (EG&G-Ortec, Oak Ridge, TN). Excitation spectra were corrected for the wavelength-dependent intensity of the excitation light source by means of a quantum counter (Rhodamine B, 4 g l^{-1} in ethylene glycol). Excitation and emission spectra of vitamin A and arachidonic acid in chlorophorm solution were also recorded with the same apparatus and used for fitting analysis, as described below.

Microspectrofluorometric analysis of liver homogenate unsoluble material remaining after organic extraction, and of single cells was performed under epi-illumination conditions by means of a Leitz microspectrograph (Wetzlar, Germany) equipped with an Optical Multichannel Analyzer (OMA, EG&G, Princeton Applied Research, Princeton, NJ), mounting a Jarrell-Ash Monospec 27 spectrograph (Allied Analytical System, Waltham, MA; mod. 82–499, H150 g mm^{-1} grating), with a 512 element intensified diode array detector (mod. 1420/512). A 100 W Hg lamp (Osram, Berlin, Germany), combined with KG1 and BG38 anti-thermal filters, was used as an excitation source. The following excitation conditions were used: 366 nm (interference filter, $T = 25\%$; 390 nm dichroic mirror, $T_{366} < 2\%$); 405 nm (interference filter, $T = 40\%$; TK 405 dichroic mirror, $T_{405} = 10\%$); 436 nm (interference filter, $T = 40\%$; TK 450 dichroic mirror, $T_{436} < 2\%$); 480 nm (interference filter, $T = 40\%$; TK 515 nm dichroic mirror, $T_{436} < 2\%$).

The liver homogenate unsoluble material collected after organic extraction was put on a slide to be submitted to microspectrofluorometric analysis, using a 25X PL Fluotar Leitz objective (N.A. 0.60).

For single cell autofluorescence analysis slides were mounted up-down in a chamber with two ports, which allowed medium exchange. The chamber was filled with the Krebs–Henseleit buffer for untreated and reoxygenated/rewarmed cells, and with the N_2-saturated cold UW solution for hypoxic condition. To avoid photobleaching and possible negative effects of irradiation, at microscope, cells were centred under low intensity tungsten lamp, and only one measurement was performed for each cell. The spectrofluorometric measurements were performed by means of an oil-immersion 95X Neofluar Leitz objective, with incorporated iris diaphragm (NA 1.10–1.32). Cell autofluorescence measurements were taken on fixed areas (60 μm^2) of the cell cytoplasm, to give an estimation of the fluorophore's concentration per cell area unit. Emission spectra were recorded in the visible range, the starting wavelength

being chosen according to the excitation wavelength used. Each spectral acquisition lasted for 10 sequential scans of 200 ms each, for a total measuring time of 2 s.

Spectral fitting analysis

Autofluorescence spectra recorded on the hepatocytes were submitted to a curvefitting analysis to evaluate the relative contribution of each fluorophore involved in the overall emission. Before fitting, spectra were corrected for the set-up response, and converted into wave-number units, supposing an in-homogenous line broadening in frequency. Analysis was performed by means of an iterative non-linear curve-fitting procedure (PeakFit, SPSS Science, Chicago, IL) based on the Marquardt–Levenberg algorithm,[23] through the finding of the true absolute minimum value of the sum of squared deviations (χ^2). A linear combination of GMG (half-Gaussian modified Gaussian) spectral functions was used. For each single, pure fluorophore, GMG functions were obtained after subsequent adjustments, to match the best fit for the line shape of the experimental spectrum. The GMG function parameters were then used to estimate the relative contribution of each single spectral component to the whole fluorescence emission: after a first subjective matching of the contribution of the individual GMG bands, the fit of the spectral components was adjusted and verified by the iterative process, until a satisfying goodness of fit was obtained, according to both r^2 and residual analysis.

Spectra of pure fluorophores were obtained under the same experimental conditions used for single cell autofluorescence analysis, as already described.[1] The reference spectra of NADH, FAD, vitamin A and arachidonic acid were obtained from the solutions previously described. The reference spectrum for lipopigments was obtained from rat brain tissue, according to Armstrong *et al.*[24] As to protein contribution, a minor function at wavelengths shorter than 450 nm was considered.[13] The spectral functions describing the emission profiles of the single fluorophores are shown in Fig. 1.

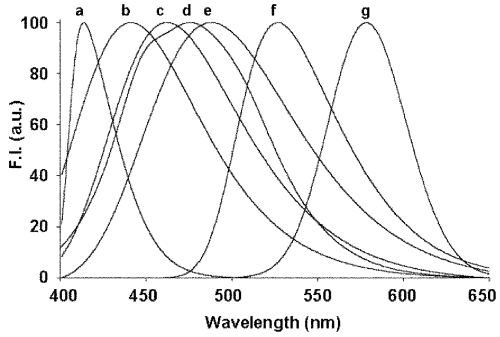

Fig. 1 Emission spectrum functions of the fluorophores used for autofluorescence fitting analysis: (a) proteins; (b) NAD(P)H in the free and (c) in the bound form; (d) fatty acids; (e) vitamin A; (f) flavins; (g) lipopigments. Curves are normalized to the peaks' amplitudes.

Results

Spectral analysis of homogenates

The aqueous phase of liver tissue homogenates showed well defined excitation bands whose peak position was dependent on the measuring wavelength. In particular, bands at about 280, 340, and 380 + 460 nm, were recorded at the measuring wavelengths of 440, 470, and 525 nm, respectively (Fig. 2A). These spectral features are very similar to the typical excitation profiles described in the literature for proteins, NAD(P)H, and flavins.[8,25,26]

Excitation at 280 nm resulted in a main emission band centered at 350 nm, attributable to proteins, and a wide tail in the 400–540 nm region. Excitation at 366 nm gave rise to a broad emission band at 430–540 nm, corresponding to

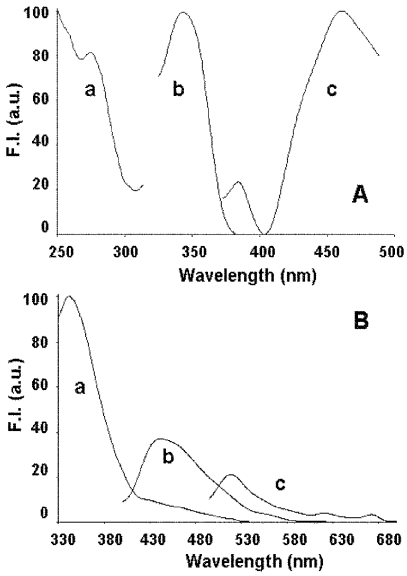

Fig. 2 Fluorescence properties of liver homogenate aqueous phase. (A) Excitation spectra were recorded at 440 (a), 470 (b) and 525 nm (c). Spectra are corrected for the set-up response and normalized to peak amplitude. (B) Emission spectra under excitation at 280 (a), 366 (b) and 470 nm (c).

the emission regions of NAD(P)H (440–480 nm) and flavins (520 nm). Excitation at 470 nm evidenced a main band centered at about 520 nm, corresponding to the emission of flavins, and two minor bands at about 625 and 670 nm, that may be ascribed to the presence of porphyrins and Heme metabolism-related compounds (Fig. 2B).

The organic phase of liver homogenate showed an excitation band in the 300–380 nm region when measured at 480 nm (Fig. 3A). This excitation band fitted with the convolution of the excitation spectra of two non-polar fluorophores, vitamin A and arachidonic acid. Vitamin A exhibits a wide excitation band peaked at about 340 nm. Arachidonic acid exhibits a more structured excitation spectrum with two main bands centered at about 315 and 350 nm with a shoulder at about 300 nm. The organic phase homogenate excitation spectrum did not show appreciable shape changes when measured at 440, 470 and 525 nm. Fitting analysis of the emission spectrum under excitation at 366 nm confirms the contribution of vitamin A and arachidonic acid to the fluorescence of the organic phase homogenate (Fig. 3B).

The tissue remnants collected after organic extraction showed different emission bands depending on the excitation wavelength (Fig. 4). Excitation at 366 nm evidenced two well defined bands centered at about 460 and at 520 nm. The former may be attributed to the tail of protein emission modified according to the profile of the excitation barrier filter. The emission at 520 nm was evidenced also by excitation at 405 and 436 nm, and can be tentatively attributed to protein-bound flavins and lipopigments. The emission in the 535–650 nm region induced by 480 nm excitation is consistent with the presence of lipopigments and phospholipids.[8,27,28]

Lipopigments are a heterogeneous group of insoluble substances characterized by a fluorescence emission at wavelengths longer than 500 nm, with spectral profiles dependent on their oxidation and polymerisation degrees.[27–28]

All the excitation conditions produced a further emission band of different amplitudes at wavelengths longer than 650 nm, which can be attributed to heme catabolism related porphyrin derivatives.[29,30]

Microspectrofluorometric cell analysis

The autofluorescence properties of single isolated hepatocytes were analysed under 366 nm excitation, that is at a wavelength in-

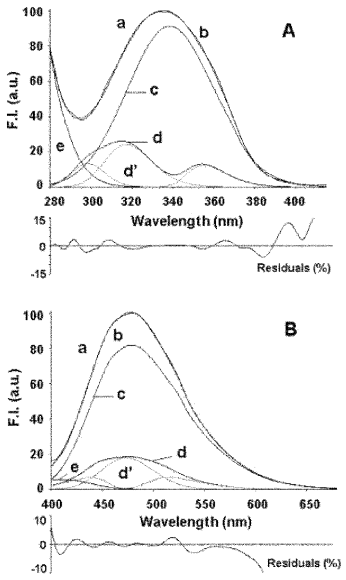

Fig. 3 Fitting analysis of fluorescence excitation (A, recorded at 480 nm) and emission (B, excited at 366 nm) spectra recorded on the liver homogenate organic phase. The curves measured (a) and generated by means of fitting procedure (b) are shown, along with the GMG functions representative of the best fitting for the emission of pure vitamin A (c), pure arachidonic acid (d), and proteins (e). Single GMG functions contributing to the arachidonic acid spectrum are also shown (d′, grey lines). Fitting analysis gave an estimation of the contributions of vitamin A, arachidonic acid, and proteins of about 67, 19 and 15%, respectively, for excitation spectrum, and of about 78, 17 and 3%, respectively, for emission spectrum. The results of residual analysis are shown at the bottom of each spectral presentation. Fitting r^2 coefficient of determination: 0.998 (A); 0.997 (B).

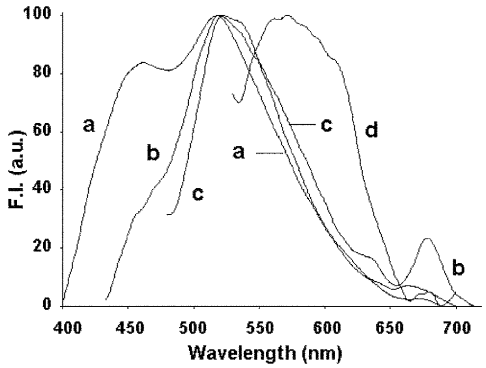

Fig. 4 Emission spectra obtained by microspectrofluorometric analysis of the tissue remnants collected after organic extraction of liver tissue homogenates, under excitation at 366 (a), 405 (b), 436 (c), and 480 nm (d). The spectra are corrected for the set-up response and normalized to the peak amplitude.

volving the most part of the endogenous fluorophores, although to a different extent.

The autofluorescence was investigated on cells under the following experimental conditions: cells isolated from the tissue, kept in Williams E medium and let to adhere to the slides (reference condition); during incubation in hypoxic UW solution at 4 °C (cold hypoxia); at 1 h of incubation in oxygenated Williams E medium at 37 °C after 20 h of cold hypoxia (rewarming–reoxygenation condition). The applied experimental conditions induced changes both in intensity and spectral shape of the cell autofluorescence emission. With respect to the reference condition (100%), the early phase of cold hypoxia was characterized by an immediate, marked increase in the whole emission signal, up to 160% after 1 h. This was followed by a slow decrease down to about 60% at 20 h of hypoxia, and by a further, faster decrease to about 50% at the end of the rewarming–reoxygenation treatment. The time course of fluorescence intensity is shown in Fig. 5.

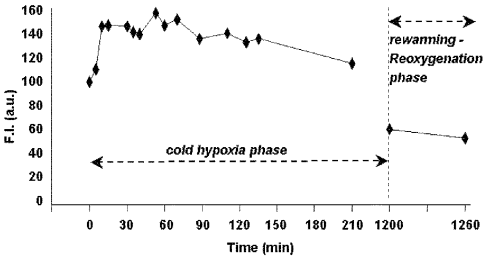

Fig. 5 Time course of the whole fluorescence emission intensity evaluated on single isolated hepatocytes: reference condition ($t = 0$), cold hypoxia (4 °C; $t = 5$ min–20 h), rewarming–reoxygenation (37 °C; $t = 20$–21 h). Each point of the curves is the mean of three independent experimental sets, with a minimum of 5 cells measured for each time point, per experiment. SE $\leq$ 5%.

Fitting analysis showed that autofluorescence emission of isolated hepatocytes is to be ascribed to the contributions of bound and free NAD(P)H, vitamin A, flavins and fatty acids, namely arachidonic acid (Fig. 6). A very good fit of the fluorescence spectra was obtained by considering an additional function at wavelengths shorter than 440 nm, plausibly attributable to the emission tail of proteins. Changes in both absolute and relative contributions of the single fluorophores to the overall emission occurred, depending on the experimental conditions considered. The results at key time points (reference condition, cold hypoxia, and rewarming–reoxygenation) are summarized in Table 1.

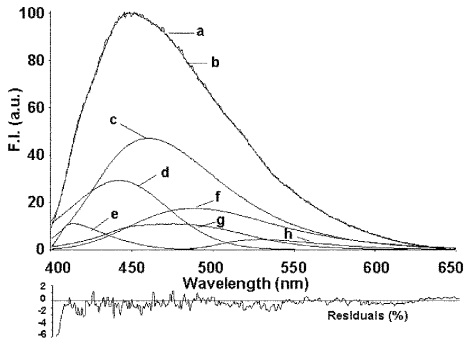

Fig. 6 Curve fitting analysis of a spectrum recorded from single isolated living hepatocytes. The curves refer to: measured spectrum (a), spectrum generated by the fitting analysis (b), NAD(P)H in the free (c), and bound (d) forms, proteins (e), vitamin A (f), arachidonic acid (g), and flavins (h). The results of residual analysis are shown at the bottom of each spectral presentation. Fitting r^2 coefficient of determination = 0.998.

The time-course of the changes in the absolute contribution of each fluorophore is shown in Fig. 7. The first phase of rising in the autofluorescence signal during cold hypoxia can be mainly ascribed to the marked increase in the absolute contributions of NAD(P)H, in the bound and in the free form. An increase occurs also for oxidised flavins, which is followed by a temporary decrease and a new increase after two hours. An initial increase is also observed for fatty acids and vitamin A. At the longest time of cold hypoxia considered (20 h), the overall signals of all fluorophores decrease; a further slight decrease is observed after rewarming–reoxygenation.

A decrease of both cells eosinophilia (data not shown) and PAS-reactivity (Fig. 8) indicate a loss respectively of cell protein and glycogen during the preservation phase.

The changes in the relative contributions of bound and free NAD(P)H, and of oxidized flavins can mirror the alteration of redox state of the cells. Ratios calculated between bound and free NAD(P)H values increased soon after cold hypoxia, the maximum being found at 1 h of cold hypoxia, followed by a slow decrease at the end of the rewarming phase to values

Table 1 Fitting analysis of hepatocytes average spectra, from three repeated, independent experimental sets[a]

Fluorophores fitting parameters	Reference condition (Williams E medium, adhered cells, 2 h)	Cold hypoxia (UW solution, 20 h)	Rewarming–reoxygenation (Krebs medium, 1 h)
NAD(P)H bound ($\lambda = 444$ nm; FWHM = 105 nm)			
Area (arbitrary units)	2573	1536	1445
Area (%)	16.60	15.64	17.10
NAD(P)H free ($\lambda = 463$ nm; FWHM = 115 nm)			
Area (arbitrary units)	6545	3094	3185
Area (%)	42.23	36.00	40.00
Flavins ($\lambda = 526$ nm; FWHM = 81 nm)			
Area (arbitrary units)	589	889	313
Area (%)	3.80	8.67	4.20
Vitamin A ($\lambda = 488$ nm; FWHM = 102 nm)			
Area (arbitrary units)	3255	2425	2028
Area (%)	21.00	23.50	21.50
Arachidonic acid (fatty acids) ($\lambda = 470$ nm; FWHM = 90 nm)			
Area (arbitrary units)	1900	1269	1098
Area (%)	12.26	12.09	13.00
Other fluorophores (Proteins) ($\lambda < 440$ nm)			
Area (arbitrary units)	637	485	380
Area (%)	4.11	4.10	4.20
Total area (arbitrary units)[b]	15499	9698	8449
Area (%)[b]	100	62	54
r^2	0.998	0.989	0.997

[a] For each experiment, a minimum of 5 cells was measured for each time point. The SD of each spectral component contribution [area (%)], calculated from the results of the curve-fitting of the averaged spectra, was $\leq 5\%$; the contribution of lipopigments was undetectable. [b] Range: 420–620 nm.

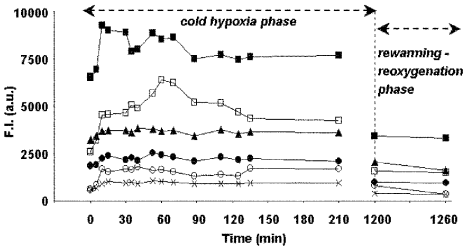

Fig. 7 Time course of the real fluorescence contribution of each single fluorophore, evaluated by means of fitting analysis on the average spectrum from three repeated, independent experimental sets. A minimum of 5 cells was measured for each time point, for each experiment. Reference condition ($t = 0$), cold hypoxia (4 °C; $t = 5$ min–20 h), rewarming–reoxygenation (37 °C; $t = 20$–21 h). A minimum of 5 cells was measured for each time point. NAD(P)H free (■), NAD(P)H bound (□), vitamin A (▲), arachidonic acid (●), flavins (○), proteins (×).

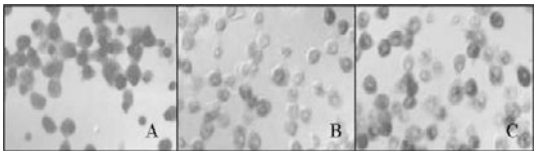

Fig. 8 Typical patterns of hepatocytes after PAS reaction for glycogen staining. (A) reference condition ($t = 0$), (B) cold hypoxia (4 °C; $t = 5$ min–20 h), (C) rewarming–reoxygenation (37 °C; $t = 20$–21 h). The presence of glycogen is revealed by the reaction positivity (dark areas).

comparable to the control. The ratio values calculated between the whole contribution of NAD(P)H, after correction for the different quantum yield of free and bound form (bound : free = 3 : 1),[31] and flavins showed an immediate drop with cold hypoxia, remained at low level during all the treatment, and increased to value similar to that of the control at the end of the rewarming phase (Fig. 9).

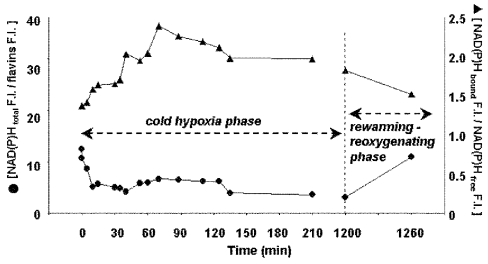

Fig. 9 Time course of $[NAD(P)H_{total}/flavins]$ (●) and of $[NAD(P)H_{bound}/NAD(P)H_{free}]$ (▲) ratio values. NAD(PH) values are corrected for the quantum efficiency of bound and free forms, 3 : 1. Reference condition ($t = 0$), cold hypoxia (4 °C; $t = 5$ min–20 h), rewarming–reoxygenation (37 °C; $t = 20$–21 h).

Discussion

Analysis of fluorescence excitation and emission spectra of liver tissue homogenates after extraction in different media indicated the presence of fluorophores with different physico-chemical nature.

Among hydrophilic compounds, the main contributions are given by proteins, NAD(P)H and flavins. The occurrence of emission bands at wavelengths longer than 650 nm indicates also the presence of porphyrin derivatives under different physico-chemical conditions, possibly related to heme catabolism.

Among the hydrophobic compounds, spectral analysis demonstrated the involvement of vitamin A and of arachidonic acid. The large contribution of vitamin A is consistent with its well established presence in both Ito cells and hepatocytes, in relation with the role of liver in the accumulation and metabolism of rethynil esters.[32] Arachidonic acid is known to be present in the liver, an organ that plays an important role in its biosynthesis from essential fatty acids, having a central position in the traffic, storage and metabolism of polyunsaturated fatty acids.[33,34] In the present work arachidonic acid, as a pure compound, was demonstrated to exhibit fluorescence

properties, despite the fact that lipids are generally considered not to be fluorescent. As a consequence, its participation as a fluorophore to the liver fluorescence cannot be neglected. Microspectrofluorometric analysis indicated also the presence of insoluble compounds such as lipopigments.

At cellular level, spectral fitting analysis demonstrated that under excitation at 366 nm the contributions of NAD(P)H, flavins, vitamin A, fatty acids and proteins account for the whole fluorescence emission of living hepatocytes. Cell autofluorescence properties were affected by the induction of the cold hypoxia condition, and the main changes concern the contributions of bound and free NAD(P)H, and of flavins. These coenzymes are fluorescent in the reduced and in the oxidized state, and their redox state is strictly dependent on the metabolic reactions in which they are involved, with particular reference to the cell energy production. As a consequence, the analysis of their fluorescence properties would allow a direct investigation of the redox state of the cells.

Hypoxia at 37 °C is reported in the literature to induce a rapid increase of fluorescence emission in isolated hepatocytes that is followed by a spontaneous decline when hypoxia is prolonged for more than 60 min.[35] This latter effect was attributed mainly to a series of events leading to a decrease in cell viability. Mitochondrial damage and a loss of NADH-enzyme association was suggested to account for the decrease in fluorescence emission, since the free NAD(P)H is known to exhibit a three times lower quantum efficiency with respect to the bound form.[31]

In our case, cell viability is preserved up to 20 h of cold hypoxia, in keeping with the slowing down of metabolic reactions by hypothermic storage and with the liver preservation efficacy of UW solution.[36] In the cold preservation phase, the low concentration of oxygen does not allow for an efficient flow of the NAD(P)H-carried electrons by the electron transfer chain in mitochondria, thus causing a temporary accumulation of reduced bound form. The subsequent slow decrease of the NAD(P)H signal suggests that – despite the low temperature, which slows down the metabolism but does not stop it completely[37] – coenzyme reoxidation takes place possibly by alternative, anaerobic pathways, such as that catalysed by lactate dehydrogenase. It is well accepted that in perfused livers carbohydrate metabolism is significantly modified by oxygen supply. In particular, glycogenolysis to lactate was described for pericentral-like hepatocytes, that is hepatocytes of the liver functional unit receiving the lowest oxygenation supply in physiological conditions.[38] In the intact organ, glycogenolysis to lactate was already reported to provide energy to the liver in anaerobic conditions.[39]

The temporal trend of the autofluorescence signals of free and bound NAD(P)H may depict the foreseeable behaviour of a cell able to adapt and survive under hypoxic conditions. As a matter of fact, it has been demonstrated that a reduction in cellular oxygen can be sensed and translated by cells into enhancing the activity of the transcription hypoxia-inducible factor 1 (HIF-1). Under hypoxic conditions HIF-1 activates genes encoding for several biomolecules, among which are the glycolitic enzymes, which produce energy from glucose in the absence of oxygen.[40,41] HIF activation by hypoxia was demonstrated in isolated hepatocytes.[42]

In our case, hypoxia might induce a fast HIF-1 activation, resulting in an enhancement of glycolytic enzymes expression, that leads to a NADH production in the cytosol (free form) through the gliceraldehyde-3-phosphate dehydrogenase reaction. Glucose used during the hypoxic period would be available from the glycogen stores, as revealed by the PAS reaction. The oxidation of NADH – required to continue the glycolytic path for ATP production under anaerobic conditions – would be allowed by lactate dehydrogenase, a further target of HIF-1.[40,41]

In general, the changes in bound/free NAD(P)H ratio may be related to the different engagement of aerobic or anaerobic pathways of NAD(P)H reoxidation, in relation with cell energy production. In fact, anaerobic reactions involve less interaction between coenzymes and enzymes than the aerobic ones, as confirmed by the loss of binding sites for NAD(P)H reported for malignant cells, where anaerobic metabolism is more favoured than in normal cells.[31,43]

Both the bound/free NAD(P)H and total NAD(P)H/flavins ratios are markedly affected during cold hypoxia. However, after the rewarming–reoxygenation phase they approach those of the reference condition, indicating that the cells successfully attempt to restore the basal redox equilibrium.

During cold hypoxia, an increase in the fluorescence contributions of both NAD(P)H and oxidized flavins is observed. This is in apparent contrast with the fact that the absence of oxygen is expected to result in an increase of the reduced forms of both coenzymes. A reduced state of flavins was reported to accompany the reduction of NAD(P)H upon impairment of hepatocyte oxidative phosphorylation by potassium cyanide, the so-called chemical anoxia.[17] The differences in the experimental conditions applied (Krebs medium, 37 °C for Thorell; UW solution, 4 °C in our case), along with the complexity of the metabolic pathways and equilibria involved may influence the cells response to the treatments. Actually, hypoxic conditions were already found to induce a transient increase in the oxidized state of flavins, that accompanied a quite immediate accumulation of NAD(P)H in the reduced form in the 3T3 cell line.[44] The reciprocal behaviour of the redox state of NAD(P)H and flavins was already defined 'bistable', to indicate its dependence on the previous metabolic steady-state.[31] In addition, the activation of alternative oxidases and the possible involvement of extramitochondrial flavins cannot be ruled out to explain our findings.

As to the other fluorophores, that is proteins, arachidonic acid, and vitamin A, the main changes consisted in a decrease of their contributions at the end of cold hypoxia. In the case of proteins, a loss of intracellular material is shown by the cytological pattern of reduced eosinophilia. Such an evidence is consistent with the starvation condition of the cells, which induces degradation of proteins, in addition to glycogenolysis – reduction of the PAS reactivity- to provide for energy production.

The decrease of arachidonic acid is consistent with the already reported loss of phospholipids from cell membranes under ischemic condition. The possible influence of the continuos balance between deacylation and reacylation of fatty acids occurring in the cells in dependence on the energetic condition may play a role, although the reactions catalyzed by phospholipase A2 and leading to the formation of arachidonic acid was shown to play a minor role in preservation/reperfusion injury to cold-stored hepatocytes.[45] The complexity of these reactions, along with the lack of detailed information on photophysical properties of different, and possibly fluorescent fatty acids, at present make the data difficult to be more clearly interpreted.

In the case of vitamin A, changes in its signal amplitude might be related to its role of antioxidant.[46] Indeed, cold-storage of hepatocytes has been shown to induce the formation of reactive oxygen species and depletion of glutathione, an intracellular antioxidant;[47,48] one cannot rule out that vitamin A is consumed along with other cellular antioxidants in order to protect hepatocytes from oxidative damage. Furthermore, one cannot exclude variation of the vitamin A fluorescence efficiency upon interaction with retinol-binding proteins. Actually, modifications both in physicochemical status and micro-environment were already reported to affect the fluorescence properties of vitamin A.[49]

The results provide the basis to develop a diagnostic technique exploiting tissue autofluorescence properties for the real time monitoring of liver functional-metabolic conditions under the different transplantation phases (work in progress).

Acknowledgements

The authors wish to thank Mr Fabrizio Rossi and Mr Gaetano Viani, Department of Internal Medicine and Therapy, University of Pavia, for the skilful laboratory technical assistance.

Work supported by CNR: Target Project 'Biotechnology' and by MIUR 'COFIN 2001'.

References

1 A. C. Croce, A. Spano, D. Locatelli, S. Barni, L. Sciola and G. Bottiroli, Dependence of fibroblast autofluorescence properties on normal and transformed conditions. Role of the metabolic activity, *Photochem. Photobiol.*, 1999, **69**, 364–374.
2 J. E. Aubin, Autofluorescence of viable cultured mammalian cells, *J. Biochem. Cytochem.*, 1979, **27**, 36–43.
3 F. W. D. Rost, *Fluorescence Microscopy*, Cambridge University Press, Cambridge, UK, vol. 2, 1995.
4 B. Chance and V. Legallais, Differential microfluorimeter for the localization of reduced pyridine nucleotide in living cells, *Rev. Sci. Instrum.*, 1959, **30**, 732–735.
5 B. Chance and B. Thorell, Localization and kinetics of reduced pyridine nucleotide in living cells by microfluorometry, *J. Biol. Chem.*, 1959, **234**, 3044–3050.
6 J. Hung, S. Lam, J. C. LeRiche and B. Palcic, Autofluorescence of normal and malignant bronchial tissue, *Lasers Med. Surg.*, 1991, **11**, 99–105.
7 R. Richards-Kortum, R. P. Rava, R. E. Petras, M. Fitzmaurice, M. Sivak and M. S. Feld, Spectroscopic diagnosis of colonic dysplasia, *Photochem. Photobiol.*, 1991, **53**, 777–786.
8 G. Bottiroli, A. C. Croce, D. Locatelli, R. Marchesini, E. Pignoli, S. Tomatis, C. Cuzzoni, S. Di Palma, M. Dal Fante and P. Spinelli, Natural fluorescence of normal and neoplastic colon: A comprehensive *ex vivo* study, *Lasers Surg. Med.*, 1995, **16**, 48–60.
9 N. Ramanujam, M. F. Mitchell, A. Mahadevan, S. Thomsen, A. Malpica, T. Wright, N. Atkinson and R. Richards-Kortum, Spectroscopic diagnosis of cervical intraepithelial neoplasia (CIN) *in vivo* using laser-induced fluorescence spectra at multiple excitation wavelengths, *Lasers Surg. Med.*, 1996, **19**, 63–74.
10 G. A. Wagnieres, W. M. Star and B. C. Wilson, *In vivo* fluorescence spectroscopy and imaging for oncological applications, *Photochem. Photobiol.*, 1998, **68**, 603–632.
11 B. Mayinger, P. Horner, M. Jordan, C. Gerlach, T. Horbach, W. Hohenberger and E. G. Hahn, Light-induced autofluorescence spectroscopy for the endoscopic detection of esophageal cancer, *Gastrointest. Endosc.*, 2001, **54**, 195–201.
12 M. Monici, G. Agati, F. Fusi, R. Pratesi, M. Paglierani, V. Santini and P. A. Bernabei, Dependence of leukemic cell autofluorescence patterns on the degree of differentiation, *Photochem. Photobiol. Sci.*, 2003, **2**, 981–987.
13 A. C. Croce, S. Fiorani, D. Locatelli, R. Nano, M. Ceroni, F. Tancioni, E. Giombelli, E. Benericetti and G. Bottiroli, Diagnostic potential of autofluorescence for an assisted intraoperative delineation of glioblastoma resection margins, *Photochem. Photobiol.*, 2003, **77**, 309–318.
14 J. J. Lemaster and R. G. Thurman, Hypoxia and reperfusion injury to liver, *Prog. Liver Dis.*, 1993, **11**, 85–114.
15 H. Jaeschke, Mechanisms of oxidant stress-induced acute tissue injury, *Proc. Soc. Exp. Biol. Med.*, 1995, **209**, 104–111.
16 C. Fan, R. M. Zwacka and J. F. Engelhardt, Therapeutic approaches for ischemia/reperfusion injury in the liver, *J. Mol. Med.*, 1999, **77**, 577–592.
17 B. Thorell, Flow-cytometric monitoring of intracellular flavins simultaneously with NAD(P)H levels, *Cytometry*, 1983, **4**, 61–65.
18 B. Vollmar, M. Burkhardt, T. Monir, H. Klauke and M. D. Menger, High resolution microscopic determination of hepatic NADH fluorescence for *in vivo* monitoring of tissue oxygenation during hemorragic shock and resuscitation, *Microvasc. Res.*, 1997, **54**, 164–173.
19 H. Klauke, T. Minor, B. Vollmar, W. Isselhard and M. D. Menger, Microscopic analysis of NADH fluorescence during aerobic and anaerobic liver preservation conditions: A noninvasive technique for assessment of hepatic metabolism, *Cryobiology*, 1998, **36**, 108–114.
20 P. Moldeus, J. Hogbderg and S. Orrenius, Isolation and use of liver cells, *Methods Enzymol.*, 1978, **52**, 60–71.
21 F. O. Belzer and J. H. Southard, Principles of solid-organ preservation by cold storage, *Transplantation*, 1988, **45**, 673–676.
22 H. U. Bergmeyer, *Methods of enzymatic analysis*, Academic Press, New York, 1965, pp. 736–743.
23 D. W. Marquardt, An algorithm for least-squares estimation of nonlinear parameters, *J. Soc. Ind. Appl. Math.*, 1963, **11**, 431–441.
24 D. Armstrong, J. Wilhelm, F. Smid and M. Elleder, Chromatography and spectrofluorometry of brain fluorophors in neuronal ceroid lipofuscinosis (NLC), *Mech. Ageing Dev.*, 1992, **64**, 293–302.
25 S. Udenfriend, *Fluorescence Assay in Biology and Medicine. Molecular Biology. An International Series of Monographs and Textbooks*, Academic Press, New York–London, 1962.
26 S. Udenfriend, *Fluorescence Assay in Biology and Medicine, Molecular Biology. An International Series of Monographs and Textbooks*, Academic Press, New York–London, 1969, vol. II.
27 M. Wolman, Lipid pigments (chromolipids): their origin, nature and significance, *Pathobiol Annu.*, 1980, **10**, 253–267.
28 A. G. E. Pearse, Pigments and pigment precursors, in *Histochemistry, Theoretical and Applied (Vol. II. Analytical Technology)*, Churchill Livingstone, Edinburgh, 1985, pp. 874–928.
29 G. Weagle, P. E. Paterson, J. Kennedy and R. Pottier, The nature of the chromophore responsible for naturally occurring fluorescence in mouse skin, *J. Photochem. Photobiol., B: Biol.*, 1998, **2**, 313–320.
30 G. Bottiroli, F. Docchio, I. Freitas, R. Ramponi and C. A. Sacchi, Spectroscopic studies of hematoporphyrin-derivative in culture medium, *Chem. Biol. Interact.*, 1984, **50**, 153–157.
31 J. M. Salmon, E. Kohen, P. Viallet, J. G. Hirscheberg, A. W. Wouters, C. Kohen and B. Thorell, Microspectrofluorometric approach to the study of free/bound NAD(P)H ratio as metabolic indicator in various cell types, *Photochem. Photobiol.*, 1982, **36**, 585–93.
32 A. V. Vieira, W. J. Schneider and P. Vieira, Retinoids: transport, metabolism, and mechanism of action, *J. Endocrinol.*, 1995, **146**, 201–207.
33 E. Cabrè and M. A. Gassul, Polyunsaturated fatty acid deficiency in liver diseases: pathophysiological and clinical significance, *Nutrition*, 1996, **12**, 542–548.
34 L. Zhou and A. Nilsson, Sources of eicosanoid precursor fatty acid pools in tissues, *J. Lipid Res.*, 2001, **42**, 1521–1542.
35 E. T. Obi-Tabot, L. M. Hanrahan, R. Cacheco, E. R. Beer, S. R. Hopkins, J. C. K. Chan, J. M. Shapiro and W. W. L. LaMorte, Changes in hepatocyte NADH fluorescence during prolonged hypoxia, *J. Surg. Res.*, 1993, **55**, 575–580.
36 J. H. Southard and F. O. Belzer, Organ preservation, *Ann. Rev. Med.*, 1995, **46**, 235–247.
37 P. A. Clavien, P. R. Harvey and S. M. Strasberg, Preservation and reperfusion injuries in liver allografts: an overview and synthesis of current studies, *Transplantation*, 1992, **53**, 957–978.
38 J. J. Lemasters and R. G. Thurman, Reperfusion injury after liver preservation for transplantation, *Annu. Rev. Pharmacol. Toxicol.*, 1997, **37**, 327–338.
39 K. Jungermann and T. Kietzmann, Oxygen: modulator of metabolic zonation and disease of the liver, *Hepatology*, 2000, **31**, 255–260.
40 P. J. Ratcliffe, J. F. O'Rourke, P. H. Maxwell and C. W. Pugh, Oxygen sensing, hypoxia-inducible factor-1 and the regulation of mammalian gene expression, *J. Exp. Biol.*, 1998, **201**, 1153–1162.
41 G. L. Semenza, HIF-1: mediator of physiological and pathophysiological responses to hypoxia, *J. Appl. Physiol.*, 2000, **88**, 1474–1480.
42 U. Roth, K. Curth, T. G. Unterman and T. Kietzmann, The transcription factors HIF-1 and HNF-4 and the coactivator p300 are involved in insulin-regulated glucokinase gene expression *via* the phosphatidylinositol 3-kinase/protein kinase B pathway, *J. Biol. Chem.*, 2004, **279**, 2623–2631.
43 T. G. V. Galeotti, D. Van Rossum, D. H. Mayer and B. Chance, On the fluorescence of NAD(P)H in whole-cell preparation of tumours and normal tissues, *Eur. J. Biochem.*, 1970, **17**, 485–496.
44 A. C. Croce, K. S. Lanza, D. Locatelli, A. Spano, S. Barni and G. Bottiroli, Microspectrofluorometric analysis of autofluorescence in cultured living cells: *in situ*, real time monitoring of energetic metabolism. *13th Int. Congress on Photobiology and 28th Annual Meeting American Society for Photobiology*, San Francisco, CA, USA, 2000. Abstract 494, p. 162.
45 J. S. Kin and J. H. Southard, Effect of phospholipases A^2 inhibitors on the release of arachidonic acid and cell viability in cold-stored hepatocytes, *Cryobiology*, 2000, **40**, 27–35.
46 E. J. Johnson, The role of carotenoids in human health, *Nutr. Clin. Care*, 2002, **5**, 56–65.
47 M. Vairetti, P. Griffini, G. Pietrocola, P. Richelmi and I. Freitas, Cold-induced apoptosis in isolated rat hepatocytes: protective role of glutathione, *Free Radical Biol. Med.*, 2001, **31**, 954–61.
48 U. Rauen and H. de Groot, Cold-induced release of reactive oxygen species as a decisive mediator of hypothermia injury to cultured liver cells, *Free Radical Biol. Med.*, 1998, **24**, 1316–1323.
49 H. Morjani, A. Beljebbar, G. D. Sockalingum, T. A. Mattioli, D. Bonnier, H. Gronemeyer and M. Manfait, Surface-enhanced Raman scattering and fluorescence spectroscopy reveal molecular interactions of all-*trans*-retinoic acid and RAR γ-ligand-binding domain, *Biospectroscopy*, 1998, **4**, 297–302.